Cerebral microbleeds may be less detectable by susceptibility weighted imaging (SWI) MRI from 24h to 72h after traumatic brain injury

Bálint S. Környei[1, 2*], Viktor Szabó[3, 1], Gabor Perlaki[4, 3, 5, 1], Bendegúz L. Balogh[2, 1], Dorottya K. Szabó Steigerwald[2, 1], Szilvia A. Nagy[4, 5, 6, 7, 1], Luca Tóth[3, 1], András Büki[3, 1], Tamas P. Doczi[3, 1], Péter Bogner[2, 1], Attila Schwarcz[3, 1], Arnold Tóth[2, 1]

[1]Medical School, University of Pécs, Hungary, [2]Department of Medical Imaging, Faculty of Health Sciences, University of Pécs, Hungary, [3]Department of Neurosurgery, Medical School, University of Pécs, Hungary, [4]MTA-PTE Clinical Neuroscience MR Research Group, Hungary, [5]Pécs Diagnostic Center, Hungary, [6]Neurobiology of Stress Research Group, Szentágothai Research Centre, University of Pécs, Hungary, [7]Department of Laboratory Medicine, Medical School, University of Pécs, Hungary

Submitted to Journal:
Frontiers in Neuroscience

Specialty Section:
Brain Imaging Methods

Article type:
Original Research Article

Manuscript ID:
711074

Received on:
17 May 2021

Revised on:
07 Aug 2021

Journal website link:
www.frontiersin.org

Conflict of interest statement

The authors declare that the research was conducted in the absence of any commercial or financial relationships that could be construed as a potential conflict of interest

Author contribution statement

Bálint Soma Környei: study conception and design, data acquisition, analysis and interpretation of data, drafting, final approval; Viktor Szabó: study design, data acquisition, draft revision, final approval; Gábor Perlaki: study design and conception, analysis and interpretation of data, draft revision, final approval; Bendegúz Balogh: analysis and interpretation of data, draft revision, final approval; Dorottya Kata Szabó Steigerwald: analysis and interpretation of data, draft revision, final approval; Szilvia A. Nagy: study design and conception, analysis and interpretation of data, draft revision, final approval; Luca Tóth: data acquisition, draft revision, final approval; András Büki: conception and design, draft revision, final approval; Tamás Dóczi: conception and design, draft revision, final approval; Péter Bogner: conception and design, draft revision, final approval; Attila Schwarcz: study conception and design, analysis and interpretation of data, draft revision, final approval Arnold Tóth: study conception and design, analysis and interpretation of data, draft revision, final approval All authors agreed to be accountable for all aspects of the work in ensuring that questions related to the accuracy or integrity of any part of the work are appropriately investigated and resolved.

Keywords

SWI MRI, Traumatic Brain Injury, Diffuse Axonal Injury, white matter, microbleeds, SWI, TMB

Abstract

Word count: 220

Purpose - A former rodent study showed that cerebral traumatic microbleeds (TMBs) may temporarily become invisible shortly after injury when detected by susceptibility weighted imaging (SWI). The present study aims to validate this phenomenon in human SWI.

Methods - In this retrospective study, 46 traumatic brain injury (TBI) patients in various forms of severity were included and willingly complied to our strict selection criteria. Clinical parameters potentially affecting TMB count, Rotterdam and Marshall CT score, Mayo Clinic Classification, contusion number and total volume were registered. The precise time between trauma and MRI (5h 19 min - 141h 54 min, including SWI and FLAIR) were individually recorded, TMB and FLAIR lesion counts were assessed. Four groups were created based on elapsed time between the trauma and MRI: 0-24h, 24-48h; 48-72h and >72h. Kruskal Wallis, ANOVA, chi square and Fisher exact tests were used to reveal differences among the groups within clinical and imaging parameters, statistical power was calculated retrospectively for each comparison.

Results- Kruskal-Wallis ANOVA with Conover post-hoc analysis showed significant ($p=0.01$; $1-\beta$ >0.9) median TMB number differences in the subacute period: 0-24h=4.00 (n=11); 24-48h=1 (n=14); 48-72h=1 (n=11); 72h< =7.5 (n=10). Neither clinical parameters nor FLAIR lesions depicted significant differences among the groups.

Conclusion- Our results demonstrate that TMBs on SWI MRI may temporarily become less detectable at 24-72 hours following TBI.

Contribution to the field

A former rodent study showed that cerebral traumatic microbleeds (TMBs) may temporarily become invisible shortly after injury when detected by susceptibility weighted imaging (SWI). The present study aims to validate this phenomenon in humans. In this retrospective study, 46 traumatic brain injury (TBI) patients in various forms of severity were included, clinical parameters potentially affecting TMB count as Rotterdam and Marshall CT score, Mayo Clinic Classification, contusion number and total volume were registered. The precise time elapsed between trauma and MRI were individually recorded, TMB and FLAIR lesion counts were assessed. Four groups were created based on elapsed time between the trauma and MRI: 0-24h, 24-48h; 48-72h and >72h. Statistical tests were used to reveal differences among the groups within clinical and imaging parameters, statistical power was calculated retrospectively for each comparison. A significant decrease of median TMB number could be revealed in the subacute period: 0-24h=4.00 (n=11); 24-48h=1 (n=14); 48-72h=1 (n=11); 72h< =7.5 (n=10). Neither clinical parameters nor FLAIR lesions depicted significant differences among the groups. Our results demonstrate that TMBs on SWI MRI may temporarily become less detectable at 24-72 hours following TBI.

Funding statement

B.S.K. was supported by the ÚNKP-20-3-I-PTE-552 New National Excellence Program of the Ministry for Innovation and Technology. A.T. was supported by the ÚNKP-20-5-PTE-794 New National Excellence Program of the Ministry for Innovation and Technology. A.T. was supported by the Bolyai Scholarship of the Hungarian Academy of Science. Sz.A.N. was supported by the ÚNKP-20-5-PTE-715 New National Excellence Program of the Ministry for Innovation and Technology and János Bolyai Research Scholarship of the Hungarian Academy of Sciences and PTE ÁOK-KA-2020-08. G.P. was supported by the János Bolyai Research Scholarship of the Hungarian Academy of Sciences and the Institutional Excellence Program for the Higher Education II within the framework of the 5th thematic program.
This study was funded by the Hungarian Scientific Research Fund Grant No. OTKA/K-120356.
Additionally, the study was also funded by EFOP-3.6.2-16-2017-00008 “The role of neuro-inflammation in neurodegeneration: from molecules to clinics”;
Supported by the ÚNKP-20-3-I-PTE-552, ÚNKP-20-5-PTE-794, and ÚNKP-20-5-PTE-715 New National Excellence Program of the Ministry for Innovation and Technology

This work was financially supported by the following grant agencies: Hungarian Brain Research Program (KTIA_NAP_13-2-2014-0019 and 2017-1.2.1-NKP-2017-00002)

Ethics statements

Studies involving animal subjects
Generated Statement: No animal studies are presented in this manuscript.

Studies involving human subjects
Generated Statement: The studies involving human participants were reviewed and approved by the Institutional Review Board of the University of Pécs (No.4525). The patients/participants provided their written informed consent to participate in this study.

Inclusion of identifiable human data
Generated Statement: No potentially identifiable human images or data is presented in this study.

Data availability statement

Generated Statement: The raw data supporting the conclusions of this article will be made available by the authors, without undue reservation.

Cerebral microbleeds may be less detectable by susceptibility weighted imaging (SWI) MRI from 24h to 72h after traumatic brain injury

Bálint S. Környei[1], Viktor Szabó[2], Gábor Perlaki[3], Bendegúz Balogh[4], Dorottya K. Szabó Steigerwald[5], Szilvia A. Nagy[6], Luca Tóth[7], András Büki[8], Tamás Dóczi[9], Péter Bogner[11], Attila Schwarcz[10] Arnold Tóth[12]

[1] Bálint Soma Környei, Department of Medical Imaging, Medical School, University of Pécs; balint.kornyei@gmail.com*[1] mailing address: UP MS Department of Medical Imaging: 7624 Pécs, Ifjúság str. 13. Office Telephone +3672/535-801

2 Viktor Szabó, Department of Neurosurgery, Medical School, University of Pécs; viktorszabo0706@gmail.com

3 Gábor Perlaki, MTA-PTE Clinical Neuroscience MR Research Group; Department of Neurosurgery, Medical School, University of Pécs; Pécs Diagnostic Center petzinger.gabor@gmail.com

4 Bendegúz Balogh, Department of Medical Imaging, Medical School, University of Pécs; bendi24@gmail.com

5 Dorottya Kata Szabó Steigerwald, Department of Medical Imaging, Medical School, University of Pécs; szabo.dorottya29@gmail.com

6 Szilvia A. Nagy, MTA-PTE Clinical Neuroscience MR Research Group, Pécs Diagnostic Center; Neurobiology of Stress Research Group, Szentágothai Research Centre, University of Pécs, Pécs, Hungary, Department of Laboratory Medicine, Medical School, University of Pécs, Pécs, Hungary; szilvia.anett.nagy@gmail.com

7 Luca Tóth, Department of Neurosurgery, Medical School, University of Pécs; tothluca.pte@gmail.com

8 András Büki, Department of Neurosurgery, Medical School, University of Pécs; buki.andras@pte.hu

9 Tamás Dóczi, Department of Neurosurgery, Medical School, University of Pécs; MTA-PTE Clinical Neuroscience MR Research Group doczi.tamas@pte.hu

11 Péter Bogner, Department of Medical Imaging, Medical School, University of Pécs; bogner.peter@pte.hu

10 Attila Schwarcz, Department of Neurosurgery, Medical School, University of Pécs; schwarcz.attila@pte.hu*[2]

12 Arnold Tóth, Department of Medical Imaging, Medical School, University of Pécs; MTA-PTE Clinical Neuroscience MR Research Group prsarn@gmail.com*2

*[1] Correspondence: Bálint Soma Környei MD balint.kornyei@gmail.com; *[2] Authors share last authorship

Key words

SWI MRI, traumatic brain injury, diffuse axonal injury, white matter, microbleeds

Abstract:

Purpose - A former rodent study showed that cerebral traumatic microbleeds (TMBs) may temporarily become invisible shortly after injury when detected by susceptibility weighted imaging (SWI). The present study aims to validate this phenomenon in human SWI.

Methods - In this retrospective study, 46 traumatic brain injury (TBI) patients in various forms of severity were included and willingly complied to our strict selection criteria. Clinical parameters potentially affecting TMB count, Rotterdam and Marshall CT score, Mayo Clinic Classification, contusion number and total volume were registered. The precise time between trauma and MRI (5h 19 min - 141h 54 min, including SWI and FLAIR) were individually recorded, TMB and FLAIR lesion counts were assessed. Four groups were created based on elapsed time between the trauma and MRI: 0-24h, 24-48h; 48-72h and >72h. Kruskal Wallis, ANOVA, chi square and Fisher exact tests were used to reveal differences among the groups within clinical and imaging parameters, statistical power was calculated retrospectively for each comparison.

Results- Kruskal-Wallis ANOVA with Conover post-hoc analysis showed significant ($p=0.01$; $1-\beta>0.9$) median TMB number differences in the subacute period: 0-24h=4.00 (n=11); 24-48h=1 (n=14); 48-72h=1 (n=11); 72h< =7.5 (n=10). Neither clinical parameters nor FLAIR lesions depicted significant differences among the groups.

Conclusion- Our results demonstrate that TMBs on SWI MRI may temporarily become less detectable at 24-72 hours following TBI.

Abbreviations

DAI	diffuse axonal injury
FA	fractional anisotropy
FA-SPM	fractional anisotropy images analyzed by statistical parametric mapping
FLIRT	FMRIB's Linear Image Registration Tool

TBI	traumatic brain injury
TMB	traumatic microbleed
UP MS	University of Pécs, Medical School

Introduction

Traumatic brain injury (TBI), has become a devastating health problem in developed countries[1][2–5]. TBI affects healthy, young, and often employed individuals resulting in a heavy burden placed on society both in sociological and economic context[3,4,6–8]. Diffuse axonal injury (DAI) caused by shear forces due to acceleration and deceleration of brain compartments of different consistency during an accident is a common pathological factor regarding TBI[9,10]. DAI has been found in all severities of TBI and is referenced as an important determining factor regarding severity and outcome[11,12]. DAI encompasses a vast spectrum, dependent upon the severity and extent of injury, which can acutely manifest as immediate loss of consciousness or confusion resulting in a coma and/or cognitive dysfunction, or in other circumstances, leads to reversible impairments to full axonal disruption[13]. A specific imaging marker regarding DAI will likely contribute to 1) early diagnosis and severity assessment, 2) timely onset of rehabilitation, 3) estimation of return to normal activity, 4) improved patient management, 5) and effectively following up on the patients' condition and assuring the efficacy of the applied therapy[14,15]. Currently, DAI is considered an exclusionary diagnosis, conventional imaging techniques are considered

not to be sensitive enough to fully visualize it[13]. Certain modern MRI techniques however are capable of detecting pathological components regarding DAI. [16,17].

Functional MRI, diffusion tensor imaging (DTI) or MR spectroscopy promises a comprehensive understanding of DAI, however, these methods are mostly applicable in form of statistical group analysis. To date, their individual routine clinical application is not entirely clarified [18–20]. T2* MRI techniques -sensitive in visualizing magnetic susceptibility- are capable of visualizing microscopic bleeding, among them, susceptibility weighted imaging (SWI) is reported to be the most sensitive [21–23].

By definition, traumatic microbleeds (TMBs) in SWI appear as ovoid or curvilinear hypointensities localized in the white matter (WM), mostly at the white-grey matter (WM-GM) junction, in the brainstem or in the corpus callosum and the region of the basal ganglia. Imaging of TMBs is indeed challenging: their visibility and number is influenced by numerous clinical and technical factors (e.g. age, SWI field strength, SWI slice thickness, TBI severity, neurological comorbidities, etc.)[24–26].

Although TMBs are reportedly potential markers of DAI[27], there is a lack of consensus regarding how DAI exactly relates to hemorrhagic lesions. A DTI study implies that DAI may develop without focal MRI lesions in TBI[19] and that DTI is also capable of revealing minute lesions of the WM and deep brain structures, which may not be visualized on T2*GRE or FLAIR images[18][28]. According to an increasing number of studies, hemorrhagic lesion localization seemingly is more important than the overall number associated with DAI severity assessment [29][30]. Based on histological analysis of one patient, a very recent study suggests DAI does not co-localize with TMBs[31]. Nevertheless,

nearly all studies concur that a certain number, form or localization of TMBs are associated with more severe injuries and less favorable outcomes, therefore their detection is of clinical importance[32–37]. Interestingly, some human case studies reported significant temporal changes regarding TMB morphology in the acute to subacute phase following injury, yet it was unclear if these changes mean only changes in appearance, or true biophysical-biochemical changes in reference to the hemorrhages. [38–42].

In our recent study, we managed to better understand this phenomenon based on a rodent cerebral microbleed model: surgically created artificial microscopic WM bleedings showed a significant and transient intensity increase (i.e. decrease in visibility) between 24-96 hours following surgery. Additionally, 69% of the lesions became "invisible," i.e., isointense to the WM which was followed by a reappearance. Histology confirmed that microbleeds were present at every time point when MRI measurements were made, therefore we regarded this phenomenon to be due to changes in biophysical properties of microbleeds. We concluded that the timing of SWI may be critical to avoid false-negative results[43]. Additionally, the relative inconsistency in previous studies regarding the clinical applicability of SWI MRI in TBI may be explained by our findings. In the present study, we aimed to reveal if such transient reduction in TMB visibility occurs in humans as well, and we aimed to define the typical time frame of this phenomenon.

Materials and Methods

Subjects

195 adults with closed TBI, compliant to our MRI protocol were initially included retrospectively from a prospectively collected observational cohort at UP Clinical Center

Department of Neurosurgery and Pécs Diagnostic Center. A crucial criterion was precise TBI time documentation. Additionally, the exact time of admission, CT and MRI acquisition were also recorded. Exclusion criteria included any diagnosis of comorbidities capable of causing WM TMBs (e.g., fat embolism, chronic hypertension, cerebral amyloid angiopathy, cavernous malformations, epilepsy, Alzheimer disease, dementia or migraine, brain tumor or cerebral metastasis [34,44–56]) based on patient medical records. Grubbs' test was applied to exclude patients with outlier TMB numbers.– Figure 3. shows our algorithm and criteria of inclusion and exclusion.

The final number of patients eventually was narrowed to 46 cases who were eligible for the study (37 male, 9 female; 6 symptomatic, 8 mild and 32 severe according to the Mayo Clinic Classification of Traumatic Brain Injury[57]). Investigations were carried out compliant to the rules of the Declaration of Helsinki, and ethical approval was granted from the Institutional Review Board of the University of Pécs (No.4525). Written informed consent was obtained from all the participants or their legally authorized representatives regarding the MRI scans used in the study.

Clinical data and admission CT parameters

TBI severity was individually defined according to the Mayo Clinic Classification of Traumatic Brain Injury (symptomatic, mild, moderate- severe)[58]. Age at the time of trauma, gender, Rotterdam[59] and Marshall CT scores[60] (assessed on admission CT), MRI field strength (1.5 or 3 T), FLAIR lesion number and macroscopic injuries were recorded. Furthermore, the total approximate volume of contusions was recorded on

admission, through individual CTs (MedView™) in accordance to the following formula developed by Rashumi U. Kothari et al.[61] (Table 1-3):

$$CV = \frac{LPD * NSL * SL}{2}$$

Where CV is the contusion voulume, LPD are the longest perpendicular diagonals of the contusion apperarin on admission CT, NSL is the number of slices on which the contusion is present and SL is slice thickness.

MRI acquisition

SWI, T1-weighted MPRAGE and FLAIR images were assessed. Brain MRI was performed using 1.5T (Avanto/Avantofit) and 3T (Magnetom Trio/Prisma Ff~~i~~t) Siemens MR scanners, and, in the case of SWI, special attention was given to the evaluation of MRI images with higher field strength and thinner slices in the estimated timeframe of TMB disappearance (24h-72h) as shown in Table 2.

T1-weighted high-resolution images were obtained using a three-dimensional (3D) MP-RAGE sequence (TI=~~900-1100~~900 ms; TR=~~1900-2530~~ 1400 ms; TE= ~~2.5-2.4~~ 3 ms; slice thickness=~~0.9~~ 1.0 mm; field of view (FOV) = ~~256~~192 ~~-~~mm*256 mm; matrix size = ~~256~~192*256. 3D and 2D FLAIR images were acquired using: TI= 18~~88.100~~-2713.4 ~~2872~~ ms; TR= 5000-~~9000~~8910 ms; slice thickness= ~~1.5~~ 4.0 mm; FOV= 192-2~~25~~30 mm*2~~25~~00-256 mm; matrix size= 187-~~512~~384*256-512, and 3D SWI images were acquired as follows: TR=~~27~~46-49 ms; TE= ~~20-~~40 ms; slice thickness=~~1.~~2.0-3.0 mm; FOV= ~~137~~158-201mm*~~230-240~~ 230 mm; matrix size= ~~125~~137-~~182~~177* ~~256~~192-~~320~~256, with no inter-slice gap for 1.5 T and (3D) MP-RAGE

sequence (TI=900 or 1100 ms; TR= 1380 or 2530 ms; TE= 2.2 or 3.4 ms; slice thickness=1.0 or 1.1 mm; FOV= 211 or 256 mm * 211 or 256 mm; matrix size = 192 or 256 * 192 or 256. 3D and 2D FLAIR images were acquired using: TI= 1800-2500 ms; TR= 5000-9000 ms; slice thickness= 0.9-4.0 mm; FOV= 193-230 mm*220 or 230 mm; matrix size= 192-512*256 or 512, and 3D SWI images were acquired as follows: TR= 27 ms; TE= 20 ms; slice thickness= 1.5 mm; FOV= 158-199 mm* 220 or 230 mm; matrix size= 167-223* 256, with no inter-slice gap for 3T measurements (Supplementary Table 1).

Elapsed time expressed as hours between the trauma and the nearest SWI imaging was recorded as follows: time of the trauma was registered according to admission documentation, recorded by the National Ambulance Service or the Emergency Department of UP MS, and the exact time of scans were documented from the MRI scans' DICOM data.

Haemorrhagic and non haemorrhagic MRI lesion detection

Anonymized CT and MRI scans were read by A.T. and B.S.K., both authors with more than six years of experience in human brain CT and MRI data processing, blinded to clinical and time-to-scan data. Final lesion counts were described as per agreement. Lesion parameters were validated by P.B., specializing in neuroradiology with more than ten years of experience.

SWI TMBs were defined as ovoid or curvilinear hypointensities localized in the WM, mostly at the WM-GM junction, in the brainstem or in the corpus callosum and the region of the basal ganglia. ~~described above~~. For precise TMB identification, exclusion of SWI

lesion mimicks (intersects of veins, bottom of sulci, calcium deposits, artefacts caused by air-tissue interfaces or macroscopic bleeding caused by e.g., an intraventricular drain) had to be performed. Therefore, SWI images were registered with high resolution T1 weighted images using FMRIB's Linear Image Registration Tool (FLIRT), which allowed a multi-modal and anatomically accurate assessment of TMBs[62–64].

Lesions adjacent to contusions, intraventricular hemorrhage or bone-air interface artifacts (e.g., near mastoid process) or an external ventricular drain, were excluded. The overall TMB number and localization according to Adams et al [65] was individually recorded.

FLAIR lesions were defined as focal, round to ovoid hyperintensities and strictly localized within the white matter.

Examples of SWI and FLAIR lesions at different time points are shown in Figure 1 and Figure 2.

~~Anonymized CT and MRI scans were read by A.T. and B.S.K., both authors with more than six years of experience in human brain CT and MRI data processing, blinded to clinical and time to scan data. Final lesion counts were described as per agreement. Lesion parameters were validated by P.B., specializing in neuroradiology with more than ten years of experience.~~

Statistical analysis

MedCalc for Windows, version 19.1.1. (MedCalc Software, Ostend, Belgium) was used regarding all statistical analyses on the anonymized data except for the Fisher exact test,

which was processed using the IBM SPSS Statistics for Windows, Version 25.0. (Armonk, NY: IBM Corp.). Descriptive statistics were applied to summarize clinical, CT and MRI data. In cases of non-normal distributed data median and the interquartile range, and in cases of normally distributed data mean and SD are depicted in Table 2.

To model temporal trends of lesions, linear, exponential and second degree polynomial trend lines were aligned to the number of SWI TMBs and FLAIR hyperintensities in function of elapsed time following TBI, respectively, Grubbs' test was applied to exclude outliers. For further analysis, the best fitting trend line (the one with highest R^2 value) was selected. For both TMBs and FLAIR lesions, a second order polynomial trend line aligned the best (R^2=0.20). The solution of this trend line's equation regarding the average TMB count defined the exact time frame in which TMB numbers were below average.

The commonly referred defined time frame was adapted considering clinical and practical applicability, thus four groups were created based on the elapsed time between the trauma and the earliest MRI: 0-24h (n=11); 24-48h (n=14); 48-72h (n=11) 72h< (n=10). Sapiro-Wilk normality test was applied to test the distribution of TMB, and FLAIR lesion numbers, age, contusion number and total volume. Fisher exact test with continuity correction was used to elucidate differences in occurrence of categorical variables between the groups possibly affecting lesion count such as gender, Mayo TBI classification, Rotterdam and Marshall scores, TMB localization, slice thickness, and scanner field strength. Kruskall-Wallis ANOVA with Conover post hoc test was applied to assess the average TMB and FLAIR lesion count, contusion number and volume differences between the groups, statistical power of the comparisons was calculated with R Statistical Software's

MultNonParam-kwpower package (version 3.6.0.; R Foundation for Statistical Computing, Vienna, Austria).

Results

According to the Mayo Classification System regarding TBI, severity distributed as 6 symptomatic, 8 mild and 32 moderate-severe in the set of 46 patients. The distribution of age in our entire set of patients was not normally distributed (p=0.02), mean age in time of the trauma was 46.09 (SD=24.39) years. A total of 248 TMBs (131 on 3T and 117 on 1.5T scanners) and 220 hyperintense focal lesions in FLAIR were identified among 46 patients. In reference to acute CTs, 16 contusions were detectable in 9 of our patients. Detailed demographic and admission clinical data are presented in Table 1-3. A second order polynomial trend line is depicted regarding the individual TMB number over time with the highest R^2 value. In reference to the TMB number R^2= 0.2; p=0.002; y=3,0206X^2-13,065X+15,04 values were yielded (Figure 4). The average TMB number with respect to the entire population was 5.4. Substituting this value in the quadratic formula:

$$x1;2 = \frac{-b \pm \sqrt{b^2 - 4ac}}{2a}$$

X_1=85h 55min, and X_2=21h 50min were yielded. The nearest two acquisitions in our set of patients to these results were 21h11min and 79h45min following trauma. This result supported a strong tendency regarding the further division of our data into the groups described in methods (0-24h (n=11); 24-48h (n=14); 48-72h (n=11) 72h< (n=10). Additionally, a polynomial tendency line was represented with the highest R^2 value for FLAIR lesion numbers (R^2=0,07 p=0.08, Figure 5).

Sapiro-Wilk normality test revealed both TMB (0-24h: p=0.003; 24-48h: p=0.005; 48-72h: p=0.003; 72h<: p=0.04) and FLAIR lesion count significantly differed from normal distribution in every group (0-24h: p=0.003; 24-48h: p= 0.004; 48-72h: p=0.003; 72h<: p=0.04) and in the entire population, as well (p<0.001 for both TMB and FLAIR lesion count). Contusion numbers did not show normal distribution (p<0.001 in every group), contusion volumes as continuous variables also failed to show normal distribution, median contusion volumes were 0-24h=842.00 (IQR 539.29-1316.00) mm^3; 24-48h= 331.50 (IQR 0.00-1642.25) mm^3; 48-72h=214.00 (IQR 143.28-9480.25) mm^3; 72h< = 129.60 mm^3. Patients' age in each group did not significantly differ from that which is normally distributed: 0-24: p=0.12; 24-48h: p=0.16; 48-72h= p=0.28; 72h< p=0.14. Results for comparison of clinical and CT data among groups were as follows: mean age in years were 0-24h=34.45 (SD=25.72); 24-48h=52.00 (SD=25.45); 48-72h=53.91 (SD=18.65); 72h< =42.00 (SD=24.59). One-way ANOVA revealed there were no significant differences in relation to age: p=0.19 (Table 2). Fisher exact test did not reveal significant differences with respect to the Mayo TBI classification (p=0.11), Rotterdam (p=0.09) and Marshall (p=0.73) scores, SWI field strength (p=0.77) and slice thickness (p=0.59), in the distribution of macroscopic pathologies (p=0.79) or the gender of our patients (p=0.72). (Table 2.). Median TMB count in each group were as follows: 0-24h=4.0 (IQR 1.50-11.00); 24-48h=1.0 (IQR 0.00-3.00); 48-72h=1.0 (IQR 0.00-6.00); >72h=7.5 (IQR 3.00-10.00), while median FLAIR lesion count was 0-24h=0,00 (IQR 0.00-1.75); 24-48h=0,50 (IQR 0.00-14.00); 48-72h=3,00 (IQR 1.00-4.00); >72h=5,00 (IQR 1.00-14.00) (Table 3). Kruskal-Wallis test for TMBs revealed significant differences (p=0,01) between the groups, but showed no significant correlations with respect to FLAIR lesions (p=0.18), number of contusions (p=0.66) or in respect to the average contusion volume (p=0.69), as it is shown in Table 3 and

Figure 6. Statistical power was 1-β>0.9 for TMB, FLAIR lesion count and contusion volume comparisons. TMB localization did not show differences amongst the groups (p=0.68).

Discussion

This retrospective study on cross-sectional imaging data enabled an indirect validation of the phenomenon of general transient TMB visibility decrease in human SWI scans. A trend line representing the individual TMB count revealed a nadir between approximately 21-80h following trauma. According to practical considerations, these time points were adjusted to 24h and 72h for further analysis. Due to the cross-sectional nature of the study, it was crucial to check the presence regarding factors potentially posing as a bias. Neither TBI severity (according to Mayo classification and Marshall score), distribution of macroscopic pathologies, SWI field strength, age, gender distribution or any of the influential factors among the time-groups significantly differed. Thus, these time-groups proved ideally suitable to examine the influence of elapsed time between TBI and SWI on TMB visibility. Median TMB count in the 24-72h period was significantly lower than in the hyperacute (0-24h) or than in the 72h< period. Although TMB formation is reported to be significantly more frequent among older patients, we experienced lower median TMB numbers in groups in which the average age was higher.

As an internal control of our study, we examined the occurrence of FLAIR lesions, as markers of edema developing along with DAI, over time. Distinctly, FLAIR lesion count did not significantly differ in the examined time period, which suggests we are confronting a

phenomenon specific for TMBs. FLAIR lesions are also regarded as markers of DAI and injury severity and may be more stable over the acute to subacute phase however, previous studies suggest they are not so specific and clearly related to the extent of actual DAI and prognosis[66–69] as TMBs[70].

Findings of this study are congruent with our former results: in our rat model, TMBs showed significant temporal visibility reduction in SWI, they often became completely invisible in the 24h-96h period, while microbleeds' consistent presence was histologically proven. Reappearance was demonstrated after 96h. In this paper, the authors expressed that the most possible explanation regarding acute TMB disappearance may be clot retraction caused by voxel level homogenization resulting in signal gain. Authors also suspected the possible role of methemoglobin formation and consequential T1 shine through. The re-appearance of microbleeds could be explained by the development of late breakdown products of hemoglobin as hemosiderin and ferritin, known to be superparamagnetic[71,72].

Our findings support former case studies reporting TMBs' morphological changes in SWI, moreover coincide with case observations by Watanabe et al, TMB invisibility may occur roughly between 24 hours and seven days after formation[40]. Furthermore, a study focusing on cerebral blood flow changes in an experimental closed head injury rat model, authors ancillary reported some cases in which hypointense foci congruent with TMBs disappeared and later reappeared[73].

The main practical consequence of these results implies SWI may be false-negative for TMBs between 24h and 72h following injury. Half of our patients (23 of 46) were examined in this time period. This demonstrates at least in our institution, there is a considerable

chance for patients being MRI scanned within the "decreased TMB visibility" period. We assume this may be a general problem, since MRI is almost always electively, secondarily performed to admission CT-s, often after clinical stabilization. Additionally, our finding may be applicable not only in relation to TMBs but to the acute examination of every pathology capable of causing WM TMBs. Although 1.5T and 3T field strength acquisition rates were rather evenly distributed among time points, considering overall lesion counts 3T detected somewhat more lesions (131) than 1.5T (117) supporting the fact 3T has a higher sensitivity for TMBs irrespective from imaging timing.

The main limitations of this study are the limited sample size, as a result of our strict inclusion criteria and temporal features of TMBs were indirectly investigated based on cross-sectional data. Also, according to the assumed nature of temporal changes of TMB visibility, there could be an uncertainty of TMB development in patients examined between 24 – 72 hours. Direct investigation of the temporal visibility changes of TMBs would have been only possible by a longitudinal study. Unfortunately, the conduction of multiple time point follow-up MRI studies in TBI, especially when including severely injured patients is almost impossible: although MRI itself can be regarded as a safe imaging technique, the relatively long acquisition time can be inconvenient for TBI patients, or may even pose risk for severely injured patients due to patient and anesthesiological/intensive care gear transportation. However, very strict patient selection criteria were applied and factors most possibly affecting TMB presence were considered to minimize biased results.

Conclusion

345 This retrospective study indirectly substantiates that short-term temporary TMB
346 visibility decrease is generally present not only in rodents, but in humans, as well. Based on
347 our results, TMB visibility decrease seems to occur from 24h to 72h following TBI. MRI for
348 detecting TMBs in this period may result in false-negative findings, leading to an under-
349 diagnosis of injury severity and false prognosis estimation.
350

Figure 1. Representative examples of TMBs in SWI images in <24h, 24-48h, 48-72h and 72h< groups. All four SWI measurements were performed on a 3T Siemens Magnetom Prisma MRI scanner. According to MAYO classification both cases (top left 21 years old male, top right 50 years old male, bottom left 64 years old male and bottom right 60 years old male) were classified as severe TBI, TMBs are indicated by red circles. In the bottom left image, hypointensity caused by the intraventricular drain is indicated by blue circle.

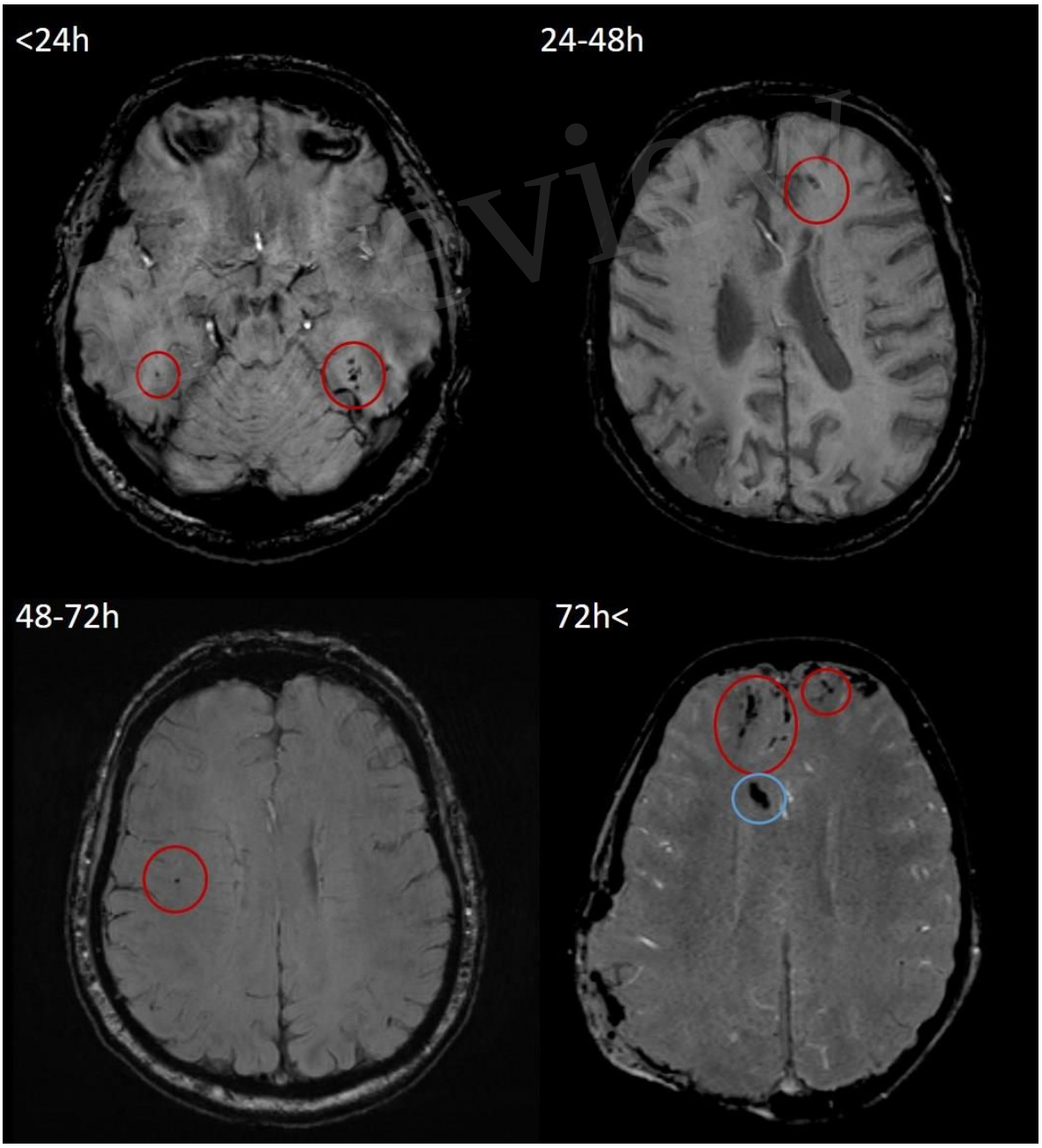

Figure 2. Representative images of non haemorrhagic/ FLAIR lesions in <24h, 24-48h, 48-72h and 72h< groups. All four FLAIR measurements were performed on a 3T Siemens Magnetom Prisma MRI scanner. According to MAYO classification, two of the for patients (top right 77 years old female, bottom left 31 years old male) suffered symptomatic TBI, two of them (top left 75 years old female, bottom right 27 years old male) were classified as severe TBI, lesions are indicated by red circles.

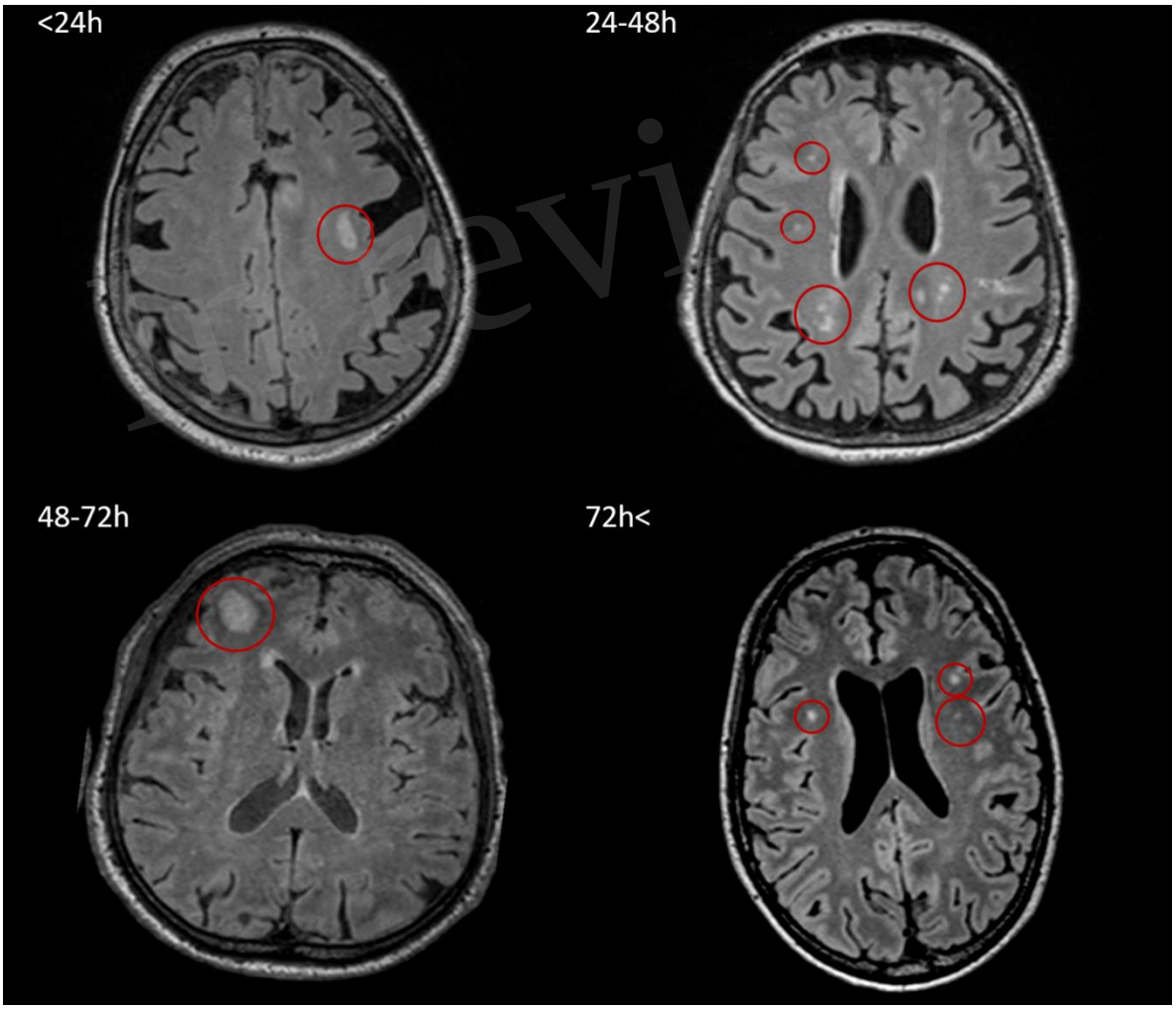

368 **Figure 3.** Algorithm of patient inclusion

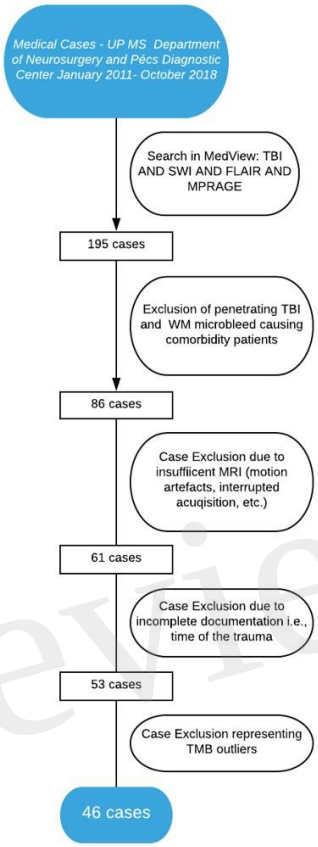

369

370 **Figure 4.** Individual TMB number over time, fitted 2nd order polynomial trend line.

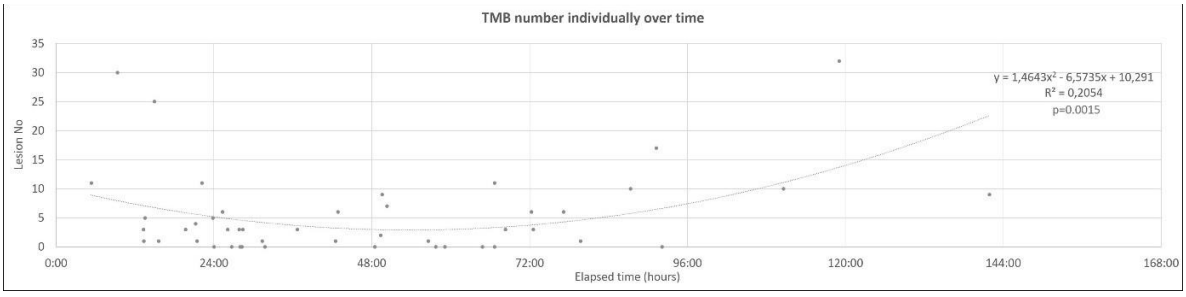

371

372

373

374

375

Figure 5. Individual FLAIR lesion number over time, representing the second order polynomial trend line.

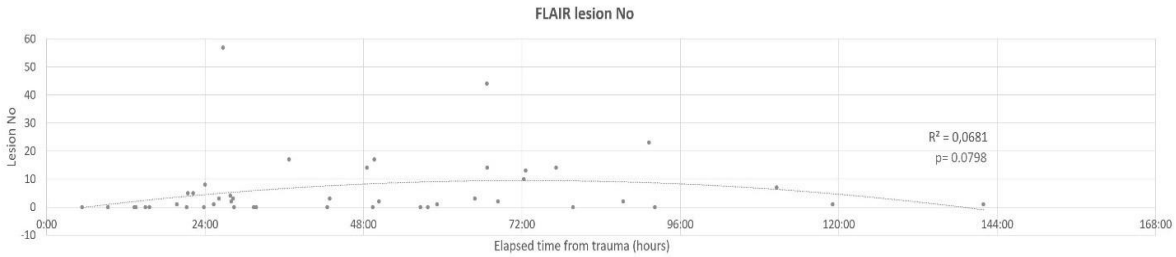

Figure 6. Kruskal-Wallis with Conover post hoc test: results for TMB number differences. "*" represents significant ($p<0.05$) differences of TMB count, the blue circe and the red square stands for the two patients with the highest TMB count.

Kruskal-Wallis test

Test statistic	10,8710
Corrected for ties Ht	11,1757
Degrees of Freedom (DF)	3
Significance level	P = 0,010813

Post-hoc analysis (Conover)

Factor	n	Average Rank	Different (P<0,05) from factor nr
(1) 0-24H	11	29,73	(2)(3)
(2) 24-48H	14	16,71	(1)(4)
(3) 48-72H	11	18,68	(1)(4)
(4) 72H<	10	31,45	(2)(3)

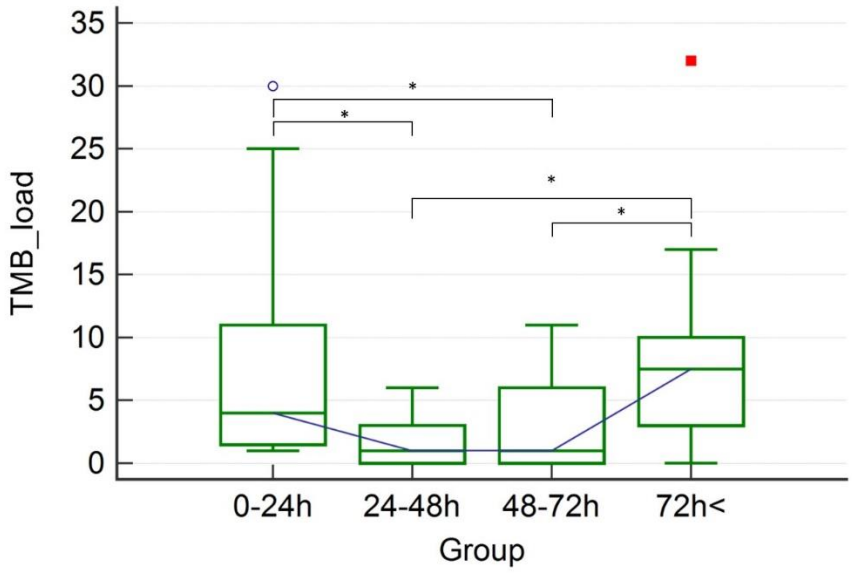

Table 1. Age, causes and symptoms of TBI according to admission data. *: Unknown, intoxicated, GM, sports, etc. **: E.g. blurred or double vision, numbness, hearing impairment, etc. ***: Disorientation, agitation, seizures, PTSD and thoracic emphysema all occurred.

			Σ	*Groups*			
				0-24h	**24-48h**	**48-72h**	**72h<**
N° patients			46	11	14	11	10
Median age for whole set of patients, mean for groups in years			50 (IQR 27-67)	34.45 (SD=25.72)	52.00 (SD=25.45)	53.91 (SD=18.65)	42.00 (SD=24.59)
Causes of TBI		falls	21	2	9	5	5
		traffic accident	15	6	2	3	4
		violence	3	1	0	2	0
		other *	7	2	3	1	1
Symptoms of tBI	*physical symptoms*	nausea/vomiting	11	2	2	4	3
		amnesia	9	1	2	5	1
		headache	7	2	0	3	2
		loss of consciousness	6	1	1	3	1
		somnolence	2	1	0	0	1
		dizziness	2	1	0	1	0
	sensory symptoms **		2	1	0	1	0
	history could not be obtained		12	3	3	3	3
	other***		7	3	1	1	2
	asymptomatic		6	0	5	0	1

Table 2. Influential factors of TMB count: age, TBI severity, and relevant SWI imaging data, level of significance of differences between groups. Results of One- Way ANOVA (*) and Fisher exact test (***).

		Σ	Groups				Significance
			0-24	24-48	48-72	72<	
N° patients		46	11	14	11	10	
Median age for whole set of patients, mean for groups in years*		50 (IQR 27-67)	34.45 (SD=25.72)	52.00 (SD=25.45)	53.91 (SD=18.65)	42.00 (SD=24.59)	p=0.19
Gender***	Male	37	10	10	9	8	p=0.72
	Female	9	1	4	2	2	
TBI severity (MAYO)***	symptomatic	6	0	3	3	0	p=0.11
	mild	8	3	0	3	2	
	moderate-severe	32	8	11	5	8	
MARSHALL score***	I	13	4	5	2	2	p=0.73
	II	8	2	2	1	3	
	III	8	2	1	4	1	
	IV	0	0	0	0	0	
	V	0	0	0	0	0	
	VI	17	3	6	4	4	
Rotterdam score***	1	27	6	12	4	5	p=0.09
	2	14	3	1	7	3	
	3	2	1	0	0	1	
	4	2	1	0	0	1	
	5	0	0	0	0	0	
	6	0	0	0	0	0	
SWI field strenght***	1.5 T	11 (23.91%)	4 (36.36%)	3 (21.43%)	2 (18.18%)	2 (20.00%)	p=0.77
	3 T	35	7	11	9	8	
SWI slice thickness (mm)***	1.15	1	1	0	0	0	p=0.59
	1.2	1	1	0	0	0	
	1.5	32	5	10	9	8	
	2	8	2	2	2	2	
	3	3	2	1	0	0	

Table 3. TMB count and localization, macroscopic pathologies, FLAIR lesion counts, contusion number and volume and the level of significance of differences between groups. Results of Kruskal-Wallis with Conover post hoc test (**) and Fisher exact test (***)

N° patients		Σ	Groups				Significance
			0-24	24-48	48-72	72<	
		46	11	14	11	10	
TMB load**	total	248	95	26	33	94	**p=0.011**
	median	3.00 (IQR 0.00-7.00)	4.00 (IQR 1.50-11.00)	1.00 (IQR 0.00-3.00)	1.00 (IQR 0.00-6.00)	7.50 (IQR 3.00-10.00)	
TMB localization***	subcortical	220	85	25	27	83	p=0.68
	corpus callosum	19	7	1	3	8	
	brainstem	9	3	0	3	3	
FLAIR lesion N°**	total	277	20	124	32	101	p=0.18
	median	2.00 (IQR 0.00-7.25)	0.00 (IQR 0.00-1.75)	0.50 (IQR 0.00-14.00)	3.00 (IQR 1.00-4.00)	5.00 (IQR 1.00-14.00)	
Contusion N°**	total	16	7	3	5	1	P=0.66
	median	0.00 (IQR 0.00-0.75)	0.00 (IQR 0.00-1.50)	0.00 (IQR 0.00-0.00)	0.00 (IQR 0.00-1.00)	0.00 (IQR 0.00-0.00)	
Contusion volume**	total	19837.8	2741.00	4064.50	12902.7	129.60	p=0.69
	median	378.25 (IQR 124.65-1446.00)	842.00 (IQR 539.29-1316.00)	331.50 (IQR 0.00-1642.25)	214.00 (IQR 143.28-9480.25)	129.60	
Macroscopic pathologies***	Intraventricular hematoma	2	1	0		1	p=0.79
	Skull fracture	13	5	5		3	
	Epidural hematoma	3	3	0		0	
	Subdural hematoma	7	1	3		3	
	Subarachnoideal hematoma	7	2	4		1	
	Atrophy	4	1	3		0	

Supplementary Table 1: MRI measurement parameters for each applied protocols.

MRI scanner / number of patients measures with protocol	T2					MPRAGE						FLAIR						SWI				
	TR	TE	SL	FOV	matrix	TI	TR	TE	SL	FOV	matrix	TI	TR	TE	SL	FOV	matrix	TR	TE	SL	FOV	matrix
3T Prisma / 31	**5500**	**106**	**4**	**220*220**	**320*320**	**1100**	**2530**	**3.4**	**1**	**256x256**	**256x256**	**(3D space,**	**5000**	**387**	**0.9**	**230x230**	**512x512**	**27**	**20**	**1.5**	**199x220**	**223x256**
1,5T Avanto / 1	6220	84	5	192*256	192*256	900	1400	3	1	192*256	192*256	1888.1	5000	99	4	192*256	384*512	46	40	3	172*230	137*192
1,5T Avanto / 1	6651	97	4	188*225	268*320	900	1400	3	1	192*256	192*256	2872.1	8750	93	4	225*225	230*256	49	40	2	180*230	158*256
1,5T Avanto / 1	6651	97	4	188*225	268*320	900	1400	3	1	192*256	192*256	2713.4	8910	93	4	195*240	187*256	49	40	2	165*230	145*256
1,5T Avanto / 1	6651	97	4	188*225	268*320	900	1400	3	1	192*256	192*256	2713.4	8910	93	4	225*225	230*256	49	40	2	180*230	158*256
1,5T Avanto / 1	6821	97	4	188*225	268*320	900	1400	3	1	192*256	192*256	2710.4	8890	93	4	225*225	230*256	49	40	2	187*230	164*256
1,5T Avanto / 1	7270	97	4	188*225	268*320	900	1400	3	1	192*256	192*256	2713.4	8910	93	4	225*225	230*256	49	40	2	201*230	177*256
1,5T Avanto / 1	7460	84	5	192x256	192x256	900	1400	3	1	192*256	192*256	1888.1	5000	99	4	192*256	384*512	46	40	3	172*230	137*192
1,5T Avanto / 1	7954	84	5	192*256	192*256	900	1400	3	1	192*256	192*256	1888.1	5000	99	4	192*256	384*512	49	40	2	201*230	177*256
1,5T Avanto / 1	8014.5	97	4	188x225	268x320	900	1400	3	1	192*256	192*256	2713.4	8910	93	4	225x225	230x256	49	40	2	180x230	158x256
1,5T Avanto / 1	8202.5	84	5	192x256	192x256	900	1400	3	1	192*256	192*256	1888.1	5000	99	4	192*256	384*512	46	40	3	158*230	125*192
3T Trio /1	6000	119	3	200x200	288x384	900	1380	2.2	1.1	211x211	192x192	2500	9000	125	3	200x200	192x256	28	20	1.2	137x230	175x320
3T Trio /1	6000	74	4	193x220	280x320	900	1380	2.2	1.1	211x211	192x192	1800	5000	93	4	193x220	224x256	27	20	1.5	173x230	182x256
3T Trio /1	6000	93	4	193*220	280*320	900	1380	2.2	1.1	211x211	192x192	1800	5000	93	4	193*220	224*256	27	20	1.5	173*230	182*256
3T Trio /1	6800	74	4	193*220	280*320	900	1380	2.2	1.1	211x211	192x192	1800	5000	93	4	193*220	224*256	27	20	1.5	173*230	182*256
3T Trio /1	6971	74	4	193*220	280*320	900	1380	2.2	1.1	211x211	192x192	1800	5000	93	4	193*220	224*256	27	20	1.5	151*230	160*256

Supplementary Figure 1. TMB count as a function of time in patients scanned by 1.5T (n=11) or 3T (n=35) scanners (y axis: TMB count; x axis: elapsed time between trauma and MRI scan individually). A 2nd order polynomial trend line could be fitted with the highest R^2 value (R^2 = 0,1318 (1.5T) and R^2 = 0,2261 (3T)) on individual TMB count in the same manner as when patients scanned with two different field strength were examined combined.

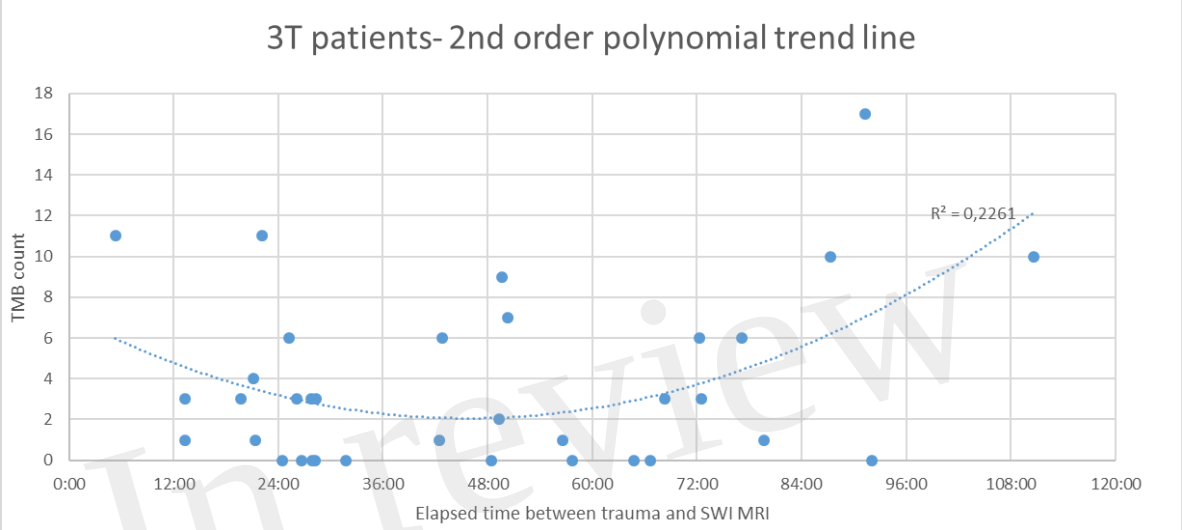

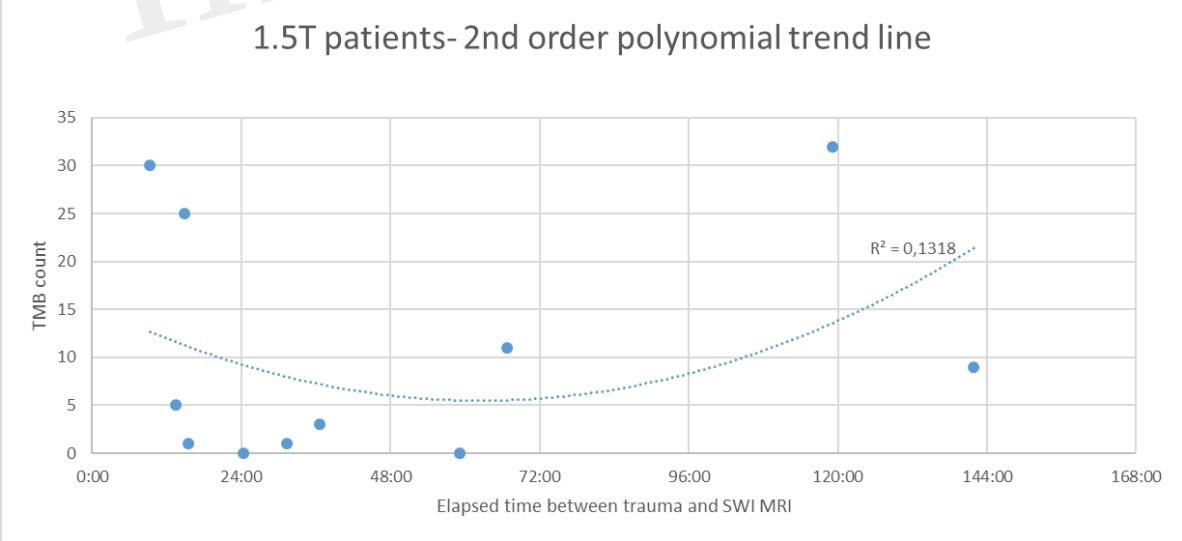

Supplementary Figure 2.: In our final 46 patients included, there were only two cases -of which one is shown in Supplementary Figure 2- when a TMB (indicated by red arrow) and a non haemorrhagic FLAIR lesion (indicated by blue arrows) were co-localised.

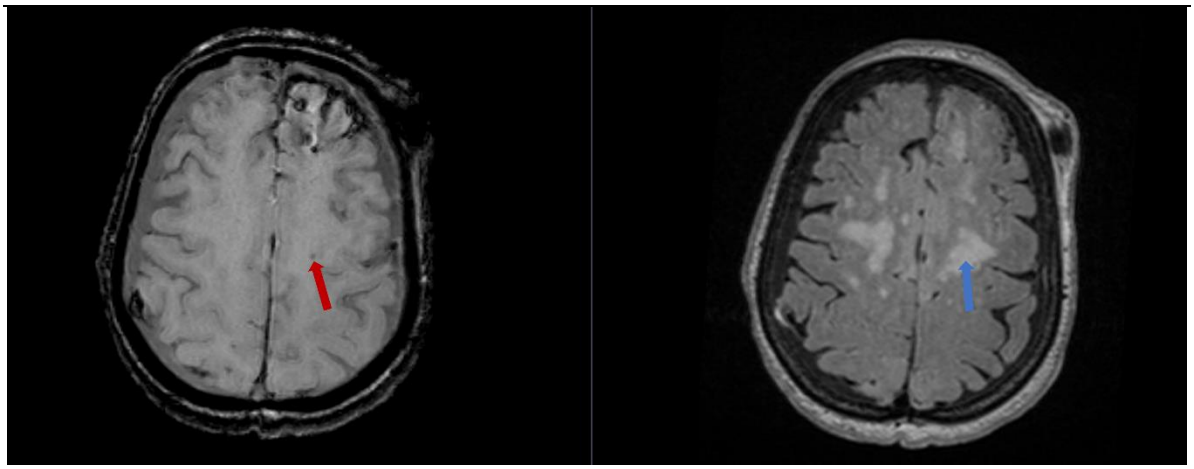

Declarations

Funding

B.S.K. was supported by the ÚNKP-20-3-I-PTE-552 New National Excellence Program of the Ministry for Innovation and Technology and the manuscript was also „PREPARED WITH THE PROFESSIONAL SUPPORT OF THE DOCTORAL STUDENT SCHOLARSHIP ROGRAM OF THE CO-OPERATIVE DOCTORAL PROGRAM OF THE MINISTRY OF INNOVATION AND TECHNOLOGY FINANCED FROM THE NATIONAL RESEARCH, DEVELOPMENT AND INNOVATION FUND. KDP-2020-986041". A.T. was supported by the ÚNKP-20-5-PTE-794 New National Excellence Program of the Ministry for Innovation and Technology. A.T. was supported by the Bolyai Scholarship of the Hungarian Academy of Science. Sz.A.N. was supported by the ÚNKP-20-5-PTE-715 New National Excellence Program of the Ministry for Innovation and Technology and János Bolyai Research Scholarship of the Hungarian Academy of Sciences and PTE ÁOK-KA-2020-08. G.P. was supported by the János Bolyai Research Scholarship of the Hungarian Academy of Sciences and the Institutional Excellence Program for the Higher Education II within the framework of the 5th thematic program.
This study was funded by the Hungarian Scientific Research Fund Grant No. OTKA/K-120356. Additionally, the study was also funded by EFOP-3.6.2-16-2017-00008 "The role of neuro-inflammation in neurodegeneration: from molecules to clinics";
Supported by the ÚNKP-20-3-I-PTE-552, ÚNKP-20-5-PTE-794, and ÚNKP-20-5-PTE-715 New National Excellence Program of the Ministry for Innovation and Technology

This work was financially supported by the following grant agencies: Hungarian Brain Research Program (KTIA_NAP_13-2-2014-0019 and 2017-1.2.1-NKP-2017-00002)

Conflicts of interest

The authors have no relevant financial or non-financial interests to disclose.

Availability of data and material

Raw data were generated at Pécs Diagnostic Center and the Department of Medical Imaging UP Clinical Center. Derived data supporting the findings of this study are available from the corresponding author [initials] on request.

Code availability

Not applicable

Authors' Contributions

Bálint Soma Környei: study conception and design, data acquisition, analysis and interpretation of data, drafting, final approval; Viktor Szabó: study design, data acquisition, draft revision, final approval; Gábor Perlaki: study design and conception, analysis and interpretation of data, draft revision, final approval; Bendegúz Balogh: analysis and interpretation of data, draft revision, final approval; Dorottya Kata Szabó Steigerwald: analysis and interpretation of data, draft revision, final approval; Szilvia A. Nagy: study design and conception, analysis and interpretation of data, draft revision, final approval; Luca Tóth: data acquisition, draft revision, final approval; András Büki: conception and design, draft revision, final approval; Tamás Dóczi: conception and design, draft revision, final approval; Péter Bogner: conception and design, draft revision, final approval; Attila Schwarcz: study conception and design, analysis and interpretation of data, draft revision, final approval Arnold Tóth: study conception and design, analysis and interpretation of data, draft revision, final approval
All authors agreed to be accountable for all aspects of the work in ensuring that questions related to the accuracy or integrity of any part of the work are appropriately investigated and resolved.

Ethics approval

Investigations were carried out compliant to the rules of the Declaration of Helsinki, and ethical approval was granted from the Institutional Review Board of the University of Pécs (No.4525).

Consent to participate

Written informed consent was obtained from all the participants or their legally authorized representatives regarding the MRI scans used in the study.

Consent for publication

Written informed consent was obtained from all the participants or their legally authorized representatives regarding the MRI scans used in the study.

Acknowledgements

We wish to express our gratitude to Farkas Kornélia Borbásné, MD, PhD, senior lecturer of the Institute of Bioanalysis UP MS for her professional assistance in biostatistics and John Eugene Marquette for his professional linguistic assistance.

References

[1] C.D. Mathers, D. Loncar, PLoS Med. 3 (2006) e442.

[2] W.-T. Chiu, S.-J. Huang, S.-H. Tsai, J.-W. Lin, M.-D. Tsai, T.-J. Lin, W.C.W. Huang, J. Clin. Neurosci. 14 (2007) 930–5.

[3] H.T. Keenan, S.L. Bratton, Dev. Neurosci. 28 (2006) 256–63.

[4] H.J. Thompson, W.C. McCormick, S.H. Kagan, J. Am. Geriatr. Soc. 54 (2006) 1590–5.

[5] T.B. Cole, JAMA 291 (2004) 2531–2.

[6] J. Lu, A. Marmarou, S. Choi, A. Maas, G. Murray, E.W. Steyerberg, Impact and Abic Study Group, Acta Neurochir. Suppl. 95 (2005) 281–5.

[7] J. Berg, F. Tagliaferri, F. Servadei, Eur. J. Neurol. 12 Suppl 1 (2005) 85–90.

[8] F. Tagliaferri, C. Compagnone, M. Korsic, F. Servadei, J. Kraus, Acta Neurochir. (Wien). 148 (2006) 255–68; discussion 268.

[9] M.J. McGinn, J.T. Povlishock, Neurosurg. Clin. N. Am. 27 (2016).

[10] C. Moenninghoff, O. Kraff, S. Maderwald, L. Umutlu, J.M. Theysohn, A. Ringelstein, K.H. Wrede, C. Deuschl, J. Altmeppen, M.E. Ladd, M. Forsting, H.H. Quick, M. Schlamann, PLoS One 10 (2015).

[11] K. Blennow, D.L. Brody, P.M. Kochanek, H. Levin, A. McKee, G.M. Ribbers, K. Yaffe, H. Zetterberg, Nat. Rev. Dis. Prim. (2016).

[12] C.Y. Tang, E. Eaves, K. Dams-O'Connor, L. Ho, E. Leung, E. Wong, D. Carpenter, J. Ng, W. Gordon, G. Pasinetti, Transl. Neurosci. (2012).

[13] T.A. Gennarelli, J.H. Adams, D.I. Graham, in: Mech. Second. Brain Damage, Springer US, 1986, pp. 15–28.

[14] Claus-W. Wallesch, Noreen Curio, Su, Brain Inj. 15 (2001) 401–412.

[15] K. Paterakis, A.H. Karantanas, A. Komnos, Z. Volikas, J. Trauma - Inj. Infect. Crit. Care 49 (2000) 1071–1075.

[16] M.K. Blitstein, G.A. Tung, Am. J. Roentgenol. 189 (2007) 720–725.

[17] R. Sharma, S. Dearaugo, B. Infeld, R. O'Sullivan, R.P. Gerraty, J. Med. Imaging Radiat. Oncol. 62 (2018) 451–463.

[18] Y. Asano, J. Shinoda, A. Okumura, T. Aki, S. Takenaka, K. Miwa, M. Yamada, T. Ito, K. Yokoyama, Neurol. Med. Chir. (Tokyo). (2012).

[19] R. Kumar, M. Husain, R.K. Gupta, K.M. Hasan, M. Haris, A.K. Agarwal, C.M. Pandey, P.A. Narayana, J. Neurotrauma (2009).

[20] A. Toth, N. Kovacs, G. Perlaki, G. Orsi, M. Aradi, H. Komaromy, E. Ezer, P. Bukovics, O. Farkas, J. Janszky, T. Doczi, A. Buki, A. Schwarcz, J. Neurotrauma (2013).

[21] S. Mittal, Z. Wu, J. Neelavalli, E.M. Haacke, Am. J. Neuroradiol. (2009).

[22] E.M. Haacke, S. Mittal, Z. Wu, J. Neelavalli, Y.C.N. Cheng, Am. J. Neuroradiol. (2009).

[23] A.L. Cheng, S. Batool, C.R. McCreary, M.L. Lauzon, R. Frayne, M. Goyal, E.E. Smith, Stroke (2013).

[24] S.M. Greenberg, M.W. Vernooij, C. Cordonnier, A. Viswanathan, R. Al-Shahi Salman, S. Warach, L.J. Launer, M.A. Van Buchem, M.M. Breteler, Lancet Neurol. (2009).

[25] M.A. Ripoll, B. Siösteen, M. Hartman, R. Raininko, Acta Radiol. (2003).

[26] P.M. Parizel, S. Makkat, E. Van Miert, J.W. Van Goethem, L. Van den Hauwe, A.M. De Schepper, Eur. Radiol. (2001).

[27] D.I. A, L. T, A.-L. P, B. A, M. W, C. MD, J. Neurosurg. 123 (2015) 1463–1475.

[28] G. Spitz, J.J. Maller, A. Ng, R. O'Sullivan, N.J. Ferris, J.L. Ponsford, J. Neurotrauma (2013).

[29] A. Toth, B. Kornyei, N. Kovacs, T. Rostas, A. Buki, T. Doczi, P. Bogner, A. Schwarcz, Behav. Brain Res. 340 (2018).

[30] S.H. Andreasen, K.W. Andersen, V. Conde, T.B. Dyrby, O.T. Puonti, L.P. Kammersgaard, C.G. Madsen, K.H. Madsen, I. Poulsen, H.R. Siebner, J. Neurotrauma (2019).

[31] A.D. Griffin, L.C. Turtzo, G.Y. Parikh, A. Tolpygo, Z. Lodato, A.D. Moses, G. Nair, D.P. Perl, N.A. Edwards, B.J. Dardzinski, R.C. Armstrong, A. Ray-Chaudhury, P.P. Mitra, L.L. Latour, Brain (2019).

[32] S. Akoudad, F.J. Wolters, A. Viswanathan, R.F. De Bruijn, A. Van Der Lugt, A. Hofman, P.J. Koudstaal, M. Arfan Ikram, M.W. Vernooij, JAMA Neurol. (2016).

[33] S. de Haan, J.C. de Groot, B. Jacobs, J. van der Naalt, Neuroradiology (2017).

[34] B.J. Kim, S.-H. Lee, J. Stroke (2013).

[35] H.J. van der Horn, S. de Haan, J.M. Spikman, J.C. de Groot, J. van der Naalt, Brain Imaging Behav. (2018).

[36] M.H. Beauchamp, R. Beare, M. Ditchfield, L. Coleman, F.E. Babl, M. Kean, L. Crossley, C. Catroppa, K.O. Yeates, V. Anderson, Cortex (2013).

[37] E.L. Yuh, P. Mukherjee, H.F. Lingsma, J.K. Yue, A.R. Ferguson, W.A. Gordon, A.B. Valadka, D.M. Schnyer, D.O. Okonkwo, A.I.R. Maas, G.T. Manley, Ann. Neurol. 73 (2013) 224–235.

552 [38] T.P. Lawrence, P.M. Pretorius, M. Ezra, T. Cadoux-Hudson, N.L. Voets, Neurosci.
553 Lett. (2017).
554 [39] A. Toth, N. Kovacs, V. Tamas, B. Kornyei, M. Nagy, A. Horvath, T. Rostas, P. Bogner,
555 J. Janszky, T. Doczi, A. Buki, A. Schwarcz, Neurosci. Lett. 617 (2016).
556 [40] Y. Ezaki, K. Tsutsumi, M. Morikawa, I. Nagata, Acta Neurochir. (Wien). 148 (2006)
557 547–50; discussion 550.
558 [41] J. Watanabe, J. Maruya, Y. Kanemaru, T. Miyauchi, K. Nishimaki, Acta Neurochir.
559 (Wien). (2016).
560 [42] S. Kallakuri, S. Bandaru, N. Zakaria, Y. Shen, Z. Kou, L. Zhang, E.M. Haacke, J.M.
561 Cavanaugh, J. Clin. Imaging Sci. (2015).
562 [43] A. Tóth, Z. Berente, P. Bogner, B. Környei, B. Balogh, E. Czeiter, K. Amrein, T. Dóczi,
563 A. Büki, A. Schwarcz, J. Neurotrauma 36 (2019) 1670–1677.
564 [44] E.M. Haacke, Z.S. DelProposto, S. Chaturvedi, V. Sehgal, M. Tenzer, J. Neelavalli, D.
565 Kido, Am. J. Neuroradiol. (2007).
566 [45] G. Trifan, R. Gattu, E.M. Haacke, Z. Kou, R.R. Benson, Magn. Reson. Imaging (2017).
567 [46] Brain Trauma Foundation, American Association of Neurological Surgeons,
568 Congress of Neurological Surgeons, Joint Section on Neurotrauma and Critical Care,
569 AANS/CNS, S.L. Bratton, R.M. Chestnut, J. Ghajar, F.F. McConnell Hammond, O.A.
570 Harris, R. Hartl, G.T. Manley, A. Nemecek, D.W. Newell, G. Rosenthal, J. Schouten,
571 L. Shutter, S.D. Timmons, J.S. Ullman, W. Videtta, J.E. Wilberger, D.W. Wright, J.
572 Neurotrauma 24 Suppl 1 (2007) S7-13.

[47] M. Susman, S.M. DiRusso, T. Sullivan, D. Risucci, P. Nealon, S. Cuff, A. Haider, D. Benzil, J. Trauma 53 (2002) 219–23; discussion 223-4.

[48] G. Trifan, R. Gattu, E.M. Haacke, Z. Kou, R.R. Benson, Magn. Reson. Imaging (2017).

[49] Y. Nakata-Kudo, T. Mizuno, K. Yamada, K. Shiga, K. Yoshikawa, S. Mori, T. Nishimura, K. Nakajima, M. Nakagawa, Dement. Geriatr. Cogn. Disord. (2006).

[50] S. Shams, J. Martola, T. Granberg, X. Li, M. Shams, S.M. Fereshtehnejad, L. Cavallin, P. Aspelin, M. Kristoffersen-Wiberg, L.O. Wahlund, Am. J. Neuroradiol. (2015).

[51] Y. Y., K. Y., W. Y., S. H., I. N., Circulation (2016).

[52] Y. Nakagami, G. Sugihara, K. Uemura, N. Jingami, K. Ueda, R. Takahashi, T. Murai, Epilepsy and Seizure (2014).

[53] A. E.B., T. G.M., D.C. A.J., K. J., F. M.D., V.D.G. J., V.B. M.A., K. M.C., J. Headache Pain (2010).

[54] J.H. Oh, J.S. Lee, S.Y. Kang, J.H. Kang, J.C. Choi, Clin. Neurol. Neurosurg. (2008).

[55] M.H. Beauchamp, R. Beare, M. Ditchfield, L. Coleman, F.E. Babl, M. Kean, L. Crossley, C. Catroppa, K.O. Yeates, V. Anderson, Cortex (2013).

[56] M. Ayaz, A.S. Boikov, E.M. Haacke, D.K. Kido, W.M. Kirsch, J. Magn. Reson. Imaging (2010).

[57] J.F. Malec, A.W. Brown, C.L. Leibson, J.T. Flaada, J.N. Mandrekar, N.N. Diehl, P.K. Perkins, J. Neurotrauma 24 (2007) 1417–1424.

[58] J.F. Malec, A.W. Brown, C.L. Leibson, J.T. Flaada, J.N. Mandrekar, N.N. Diehl, P.K. Perkins, J. Neurotrauma (2007).

[59] A.I.R. Maas, C.W.P.M. Hukkelhoven, L.F. Marshall, E.W. Steyerberg, Neurosurgery 57 (2005) 1173–1181.

[60] (n.d.).

[61] R.U. Kothari, T. Brott, J.P. Broderick, W.G. Barsan, L.R. Sauerbeck, M. Zuccarello, J. Khoury, Stroke 27 (1996) 1304–1305.

[62] D.N. Greve, B. Fischl, Neuroimage (2009).

[63] M. Jenkinson, S. Smith, Med. Image Anal. (2001).

[64] M. Jenkinson, P. Bannister, M. Brady, S. Smith, Neuroimage (2002).

[65] J.H. Adams, D. Doyle, I. Ford, T.A. Gennarelli, D.I. Graham, D.R. Mclellan, Histopathology 15 (1989) 49–59.

[66] F. Amyot, D.B. Arciniegas, M.P. Brazaitis, K.C. Curley, R. Diaz-Arrastia, A. Gandjbakhche, P. Herscovitch, S.R. Hinds, G.T. Manley, A. Pacifico, A. Razumovsky, J. Riley, W. Salzer, R. Shih, J.G. Smirniotopoulos, D. Stocker, J. Neurotrauma 32 (2015) 1693–1721.

[67] E.D. Bigler, T.J. Abildskov, J.A. Petrie, T.J. Farrer, M. Dennis, N. Simic, H.G. Taylor, K.H. Rubin, K. Vannatta, C.A. Gerhardt, T. Stancin, K.O. Yeates, Neuropsychology 27 (2013) 438–451.

[68] C. Marquez De La Plata, A. Ardelean, D. Koovakkattu, P. Srinivasan, A. Miller, V. Phuong, C. Harper, C. Moore, A. Whittemore, C. Madden, R. Diaz-Arrastia, M. Devous, J. Neurotrauma 24 (2007) 591–598.

[69] K. Ding, C.M. De La Plata, J.Y. Wang, M. Mumphrey, C. Moore, C. Harper, C.J.

615 Madden, R. McColl, A. Whittemore, M.D. Devous, R. Diaz-Arrastia, J. Neurotrauma
616 25 (2008) 1433–1440.
617 [70] K.A. Tong, S. Ashwal, B.A. Holshouser, L.A. Shutter, G. Herigault, E.M. Haacke, D.K.
618 Kido, Radiology 227 (2003) 332–339.
619 [71] W.G. Bradley, Radiology 189 (1993) 15–26.
620 [72] A. Tó th, Z. Berente, P. ter Bogner, B. lint Kö rnyei, B. Balogh, E. Czeiter, K. Amrein,
621 T. Dó czi, A. Bü ki, A. Schwarcz, (n.d.).
622 [73] S. Kallakuri, S. Bandaru, N. Zakaria, Y. Shen, Z. Kou, L. Zhang, E. Haacke, J.
623 Cavanaugh, J. Clin. Imaging Sci. 5 (2015).
624

Figure 1.JPEG

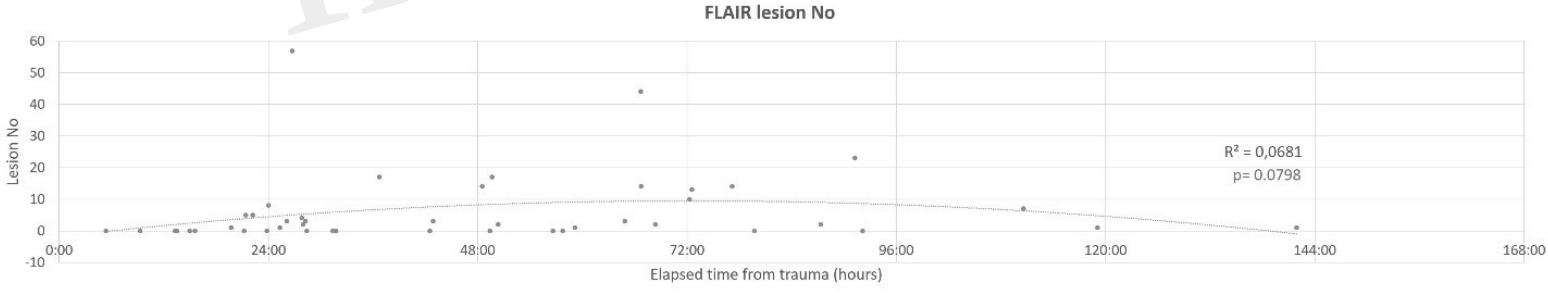

Figure 2.JPEG

Kruskal-Wallis test

Test statistic	10,8710
Corrected for ties Ht	11,1757
Degrees of Freedom (DF)	3
Significance level	P = 0,010813

Post-hoc analysis (Conover)

Factor	n	Average Rank	Different (P<0,05) from factor nr
(1) 0-24H	11	29,73	(2)(3)
(2) 24-48H	14	16,71	(1)(4)
(3) 48-72H	11	18,68	(1)(4)
(4) 72H<	10	31,45	(2)(3)

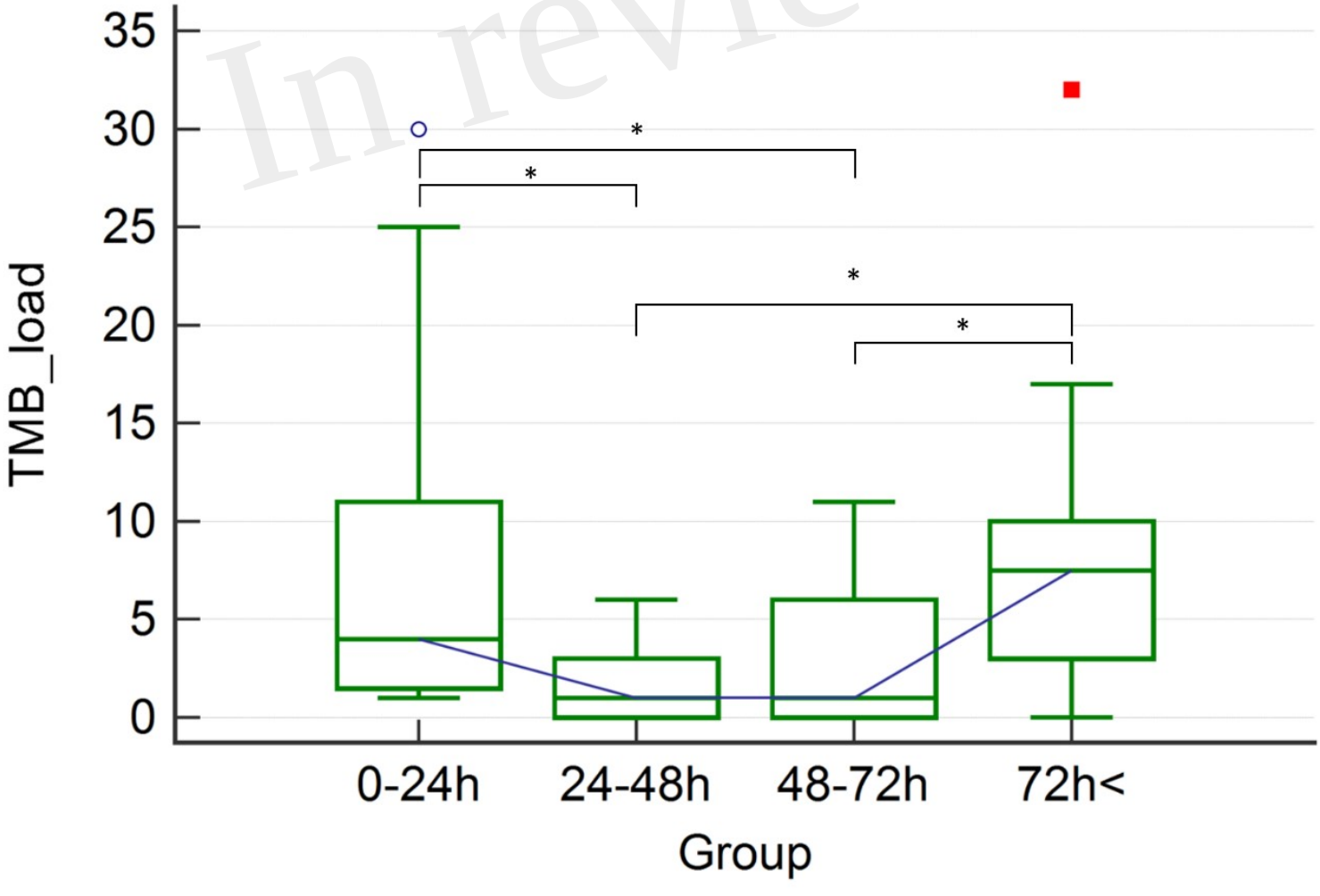

Figure 3.JPEG

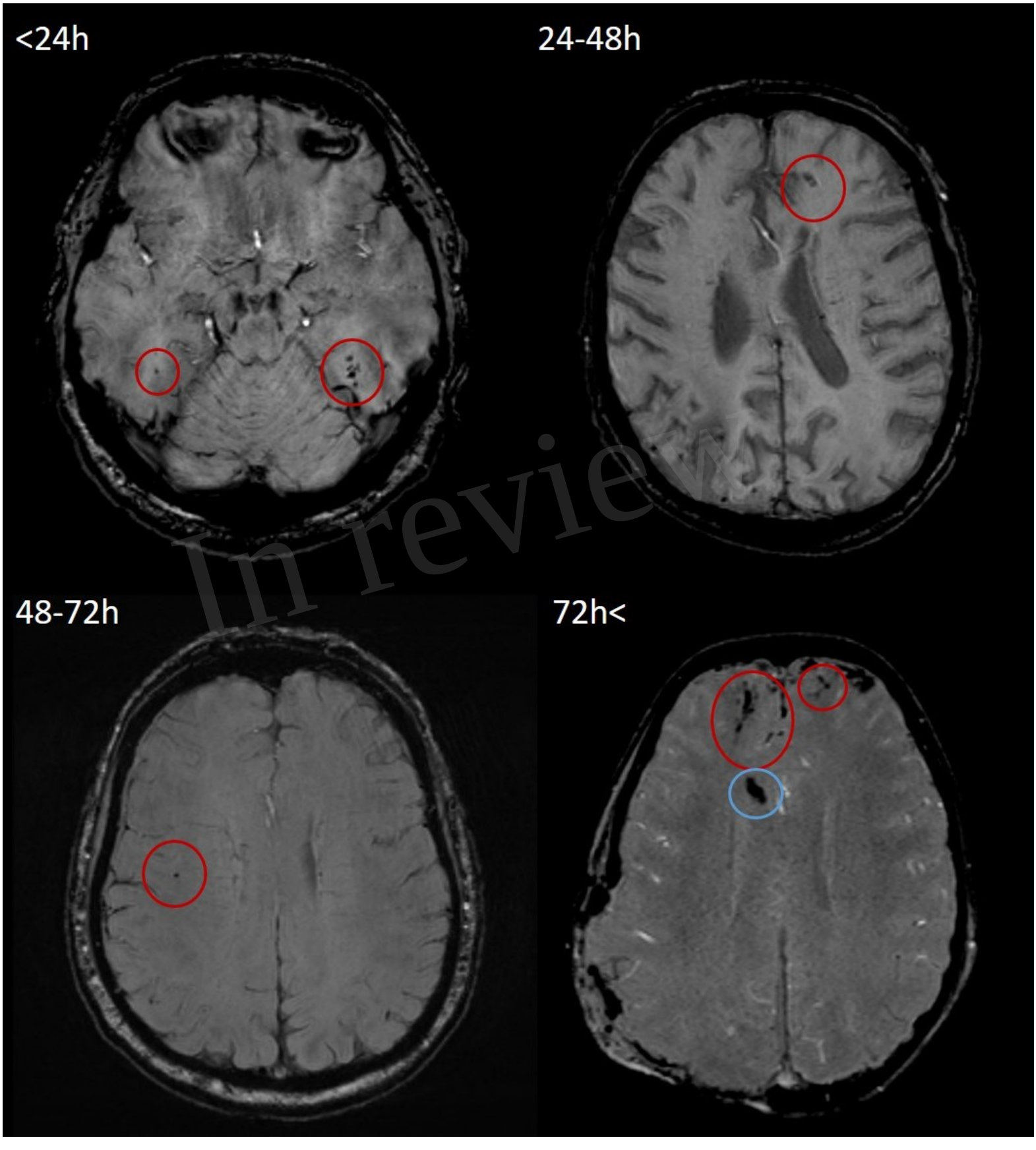

Figure 4.JPEG

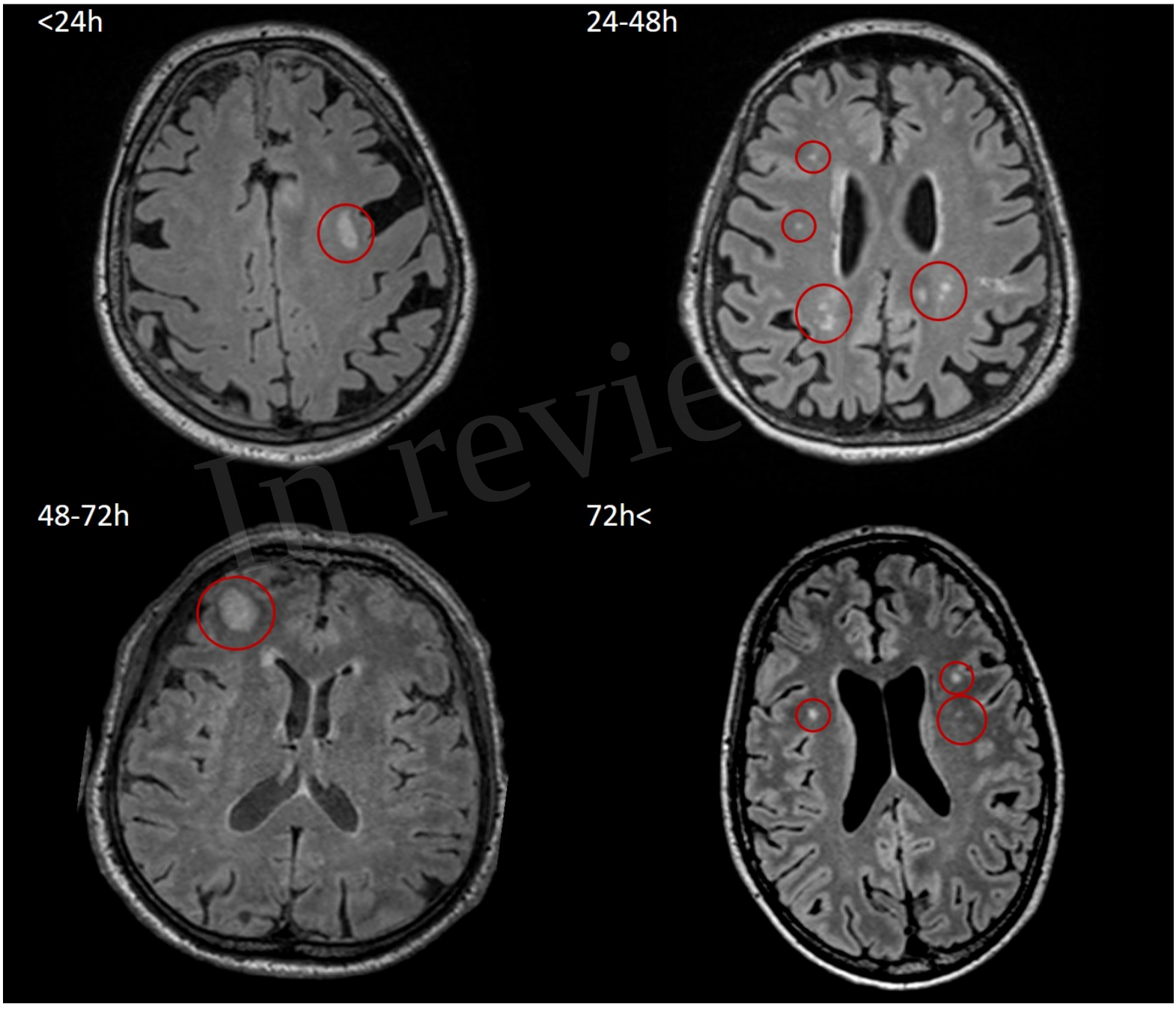

Figure 5.JPEG

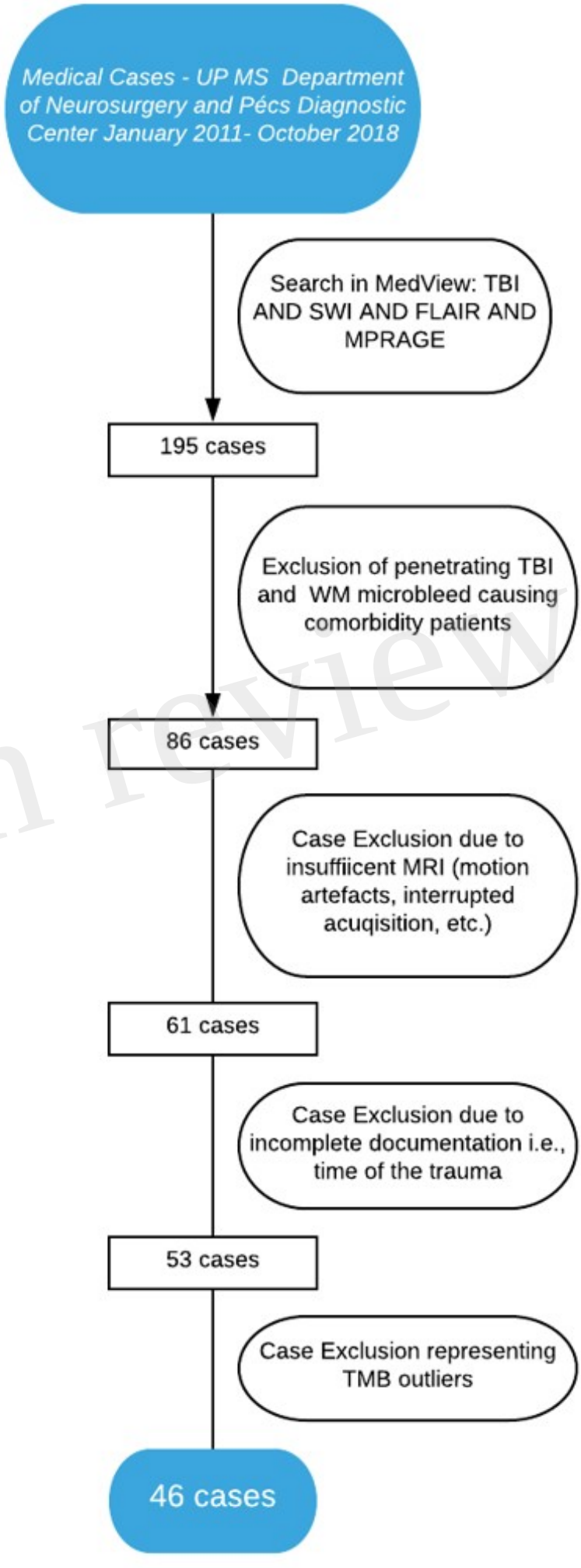

Figure 6.JPEG

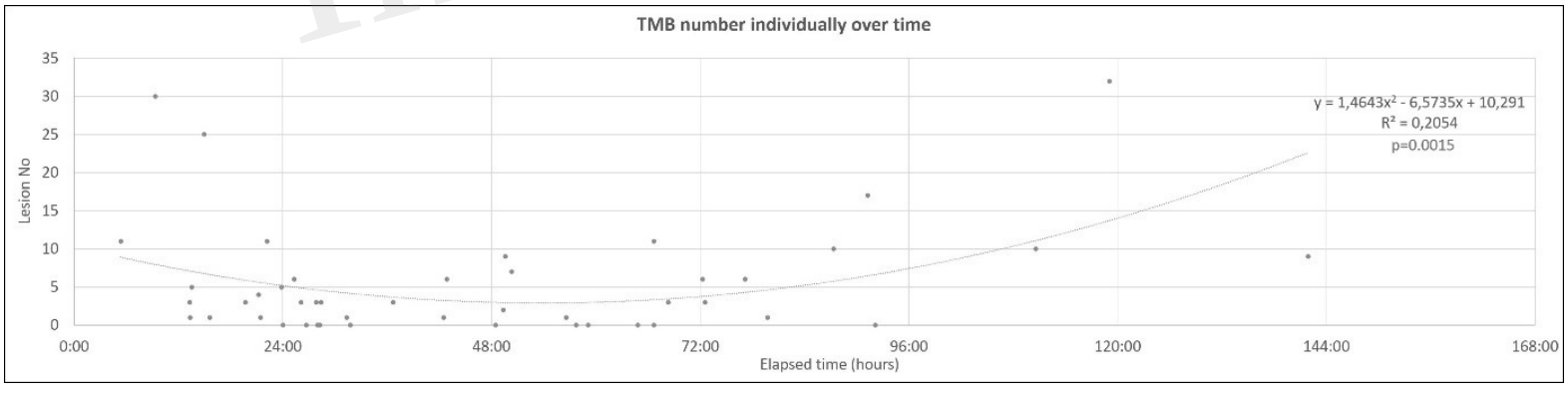

Figure 7.JPEG